# Semimetal to semiconductor transition in ErP islands grown on InP(001) due to quantum-size effects

L. Bolotov, T. Tsuchiya, and A. Nakamura
*Center for Integrated Research in Science and Engineering, and Department of Crystalline Materials Science, Nagoya University, Chikusa-ku, Nagoya 464-8603, Japan*

T. Ito, Y. Fujiwara, and Y. Takeda
*Department of Materials Science and Engineering, Nagoya University, Chikusa-ku, Nagoya 464-8603, Japan*
(Received 2 December 1998)

Thickness-dependent changes in the electronic states of semimetal ErP islands grown on the InP(001) surface by organometallic vapor-phase epitaxy have been investigated by means of scanning tunneling microscopy/spectroscopy. The normalized differential conductance spectra show a semimetal behavior for the ErP islands (20–50 nm in size) with thickness larger than 3.4 nm, while the spectra taken for the islands thinner than 3.4 nm reveal a semiconducting gap varying to ~1 eV. The thickness dependence of the observed gap is explained by the energy gap between the electron sublevel and the hole sublevel calculated using a one-dimensional square-well potential model with infinite barriers. The results demonstrate a semimetal to semiconductor transition due to the quantum size effect on the semimetal ErP band structure with a band overlap of −0.3 eV. [S0163-1829(99)01020-6]

Quantum size effects (QSE) on the energy band structure have been of great interest during the last three decades.[1–4] The progress in crystal-growth techniques has enabled us to fabricate nanometer-scale heterostructures of various materials. QSE of carriers and excitons in III-V semiconductor heterostructures has been the most extensively studied from the viewpoint of fundamental physics and from the interest for application to optical and electronic devices.[5,6] In zero-gap semiconductors, $\alpha$-Sn thin films grown on CdTe(111) with thickness of 5–8 nm have shown opening of a band gap of the order of 0.4 eV due to QSE.[7] The size quantization of electron gas in a thin metal layer at a metal-semiconductor interface has been also observed by using scanning tunneling microscopy (STM). The quantized subband energies of a $CoSi_2$ overlayer on Si(111) have been well explained by the band-structure calculation.[8] A semimetal to semiconductor transition in carbon nanoparticles with size smaller than 1 nm has been recently observed by using electron-energy-loss spectroscopy.[9] Theoretical calculations for carbon networks have predicted that the electronic states are sensitive to medium-range structural correlations due to delocalized nature of $\pi$ electrons.[10]

QSE in semimetal thin films such as Bi and Sb has been predicted by Sandomirskii in 1967.[2] A semimetal to excitonic phase transition has been also an interesting subject; when electron and hole concentrations are the same, the excitonic phase, i.e., insulating phase appears because of the Coulomb interaction between the electron and hole.[11] QSE on the semimetal band structure leads to change the carrier density as well as the band gap. Sprindt *et al.* have observed an energy gap in ultraviolet photoelectron spectra of a Sb overlayer on the GaAs(100) surface.[12] However, the energy dependence of QSE on spatial dimensions and the transition behaviors have remained unclear because of fluctuations in thickness and size of the overlayer. A study by using STM and scanning tunneling spectroscopy (STS) will enable us to resolve such problems, because electronic states on the nanometer scale can be investigated simultaneously looking at the corresponding structure. Recently, semimetal/semiconductor heterostructures of ErAs/GaAs and ErP/InP have been successfully grown by molecular-beam epitaxy[13] and organometallic vapor-phase epitaxy (OMVPE).[14] In the previous paper, we have shown the formation of nanometer-sized ErP islands with thickness of 1–4 nm and lateral size of 30–500 nm.[15] QSE in rare-earth pnictide/III-V semiconductor heterostructures is an interesting subject, because electric and magnetic properties can be modified by QSE depending upon the size on the nanometer scale.

In this paper, we report an observation of thickness-dependent changes in electronic states of ErP islands on the InP(001) surface by scanning tunneling microscopy/spectroscopy (STM/STS). The normalized differential conductance $(dI/dV)/(I/V)$ spectra show semimetal behavior for the islands thicker than 3.4 nm, while the spectra taken for the islands thinner than 3.4 nm reveal a semiconducting gap that increases up to ~1 eV. The thickness dependence of the observed gap is explained by the theoretical calculation of the one-dimensional QSE on the ErP band structure with a band overlap of −0.3 eV. These results indicates a transition from semimetal to semiconductor behavior due to QSE.

ErP islands were grown on $n^+$-InP(001) (Sn-doped) substrates by OMVPE. ErP has a rock-salt crystal structure ($a_o = 0.5595$ nm), while InP has a zinc-blende crystal structure ($a_o = 0.5869$ nm). The differences in crystal structure and lattice constant lead to the formation of strained ErP islands. The ErP layer was grown at the substrate temperatures of 530 °C and 580 °C, and the ErP coverage was controlled by changing Er-exposure duration. Details of the growth procedure are described in Ref. 14. The nominal ErP coverage was determined by Rutherford backscattering mea-

 

surements and the coverage was 3 ML for 60 min of Er-exposure duration. X-ray crystal truncation rod measurements have shown that ErP islands with a rock-salt structure were grown on the InP(001) substrate.[16] Interface mixing of compounds in the ErP/InP heterostructure hardly occurs since the diffusion constant of Er-atoms into the InP layer is as low as $1.2\times10^{-18}$ $cm^2/s$ at the growth temperature of 580 °C.[17] In the previous paper,[15] we have reported the formation of ErP islands; we can grow flat islands with size of 200–500 nm and height of 1–4 nm when the substrate temperature is 580 °C and the coverage is 3 ML.

Surface morphologies were investigated by atomic force microscopy (AFM) under ambient conditions. The STM/STS measurements in ultra-high vacuum ($\sim2\times10^{-8}$ Pa) at room temperature were carried out using a tungsten tip at a positive sample voltage of 2.5–3.5 V with a constant tunneling current of 0.1–1.0 nA. The sample was annealed at 300–350 °C for 30–50 min in the UHV chamber before the STM measurement. I-V characteristics and topographical images were simultaneously measured at various points on the surface in a current-imaging tunneling spectroscopy (CITS) mode,[18] and the I-V curves were averaged over the selected area of about $5\times5$ $nm^2$. When we changed a tip-sample distance, i.e., a value of the stabilization tunneling current, no change in the zero-current gap was observed in the I-V curve. If there exists charging of the surface due to electron propagation through the interface potential barrier between ErP and InP layers, the gap may depend on the tip-sample distance.[19] However, our results indicate that the measured I-V curves are not affected by such charging effects. Thus, the observed gap in the conductance spectra reflects electronic states of the ErP islands.

Before measuring I-V characteristics by a CITS mode, we investigated surface morphologies of ErP islands grown on the InP substrate by means of AFM and STM. Figure 1(a) shows a typical AFM image of ErP islands grown on the InP(001) surface at 580 °C and 3 ML coverage. Large islands with size of 200–500 nm are observed, and their height measured from the substrate (dark region in the AFM image) is 1–4 nm. On some ErP islands we see steps with height of 0.6–1.0 nm. We show in Fig. 1(b) a STM image of an island taken at a scan size of 176 nm×176 nm. On the island surface we see misfit dislocations and voids running parallel to the $[1\bar{1}0]$ direction of the InP substrate. Flat regions with different thicknesses are bounded by dislocations and monolayer steps, and their size is 8–50 nm. Generation of dislocations and voids partially releases the tensile strain due to the lattice mismatch of 4.67% between the ErP layer and the InP substrate.[20] The dislocation generation parallel to the $[1\bar{1}0]$ direction supports the crystalline nature of ErP islands. Figure 2(a) shows a cross-sectional profile of the topographical image along the *A*-*B* line in Fig. 1(b). We see two flat regions indicated by arrows of (a)-(b) and (c)-(e). Corresponding heights measured from the void bottom, which is the InP buffer layer, are $1.75\pm0.15$ nm (6.2 ML) and $2.30\pm0.15$ nm (8.2 ML). The height difference of these flat regions corresponds to the 2 ML thickness of ErP (0.5595 nm). The size of the highest top region along the *A*-*B* line is ~50 nm.

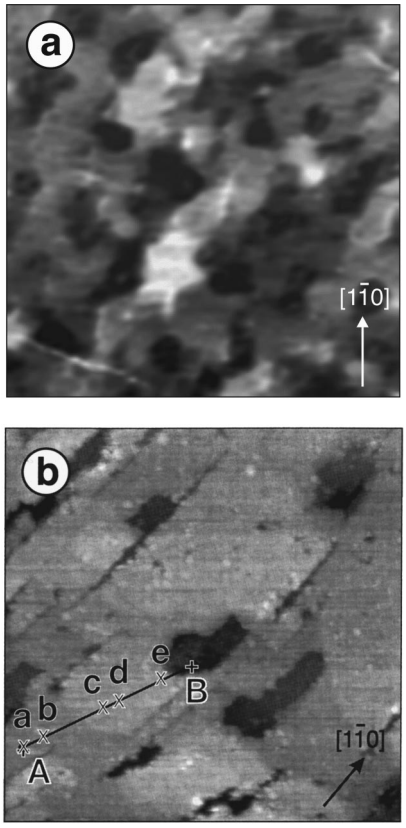


FIG. 1. (a) AFM image ($1\times1$ $\mu m^2$) of ErP islands grown on InP(001). The grayscale is 3.2 nm. (b) STM image ($176\times176$ $nm^2$) of a ErP island taken at the sample bias of +2.5 V and 0.5 nA. The gray scale is 4.2 nm.

The electronic structure of the ErP islands was investigated by STS in the CITS mode. From the measured I-V curves we calculate normalized differential conductance $(dI/dV)/(I/V)$ spectra. The measured $(I/V)$ spectrum was fitted to the exponential function and the differential conductance $(dI/dV)$ was normalized by the fitted curve. We can eliminate a numerical divergence in $(dI/dV)/(I/V)$ spectrum that occurs in the band gap region since the tunnel current is as small as the detection limit at the corresponding voltage.[21,22] To extract gap energies from $(dI/dV)/(I/V)$ spectra we used Feenstra's method;[22] we determine a gap by

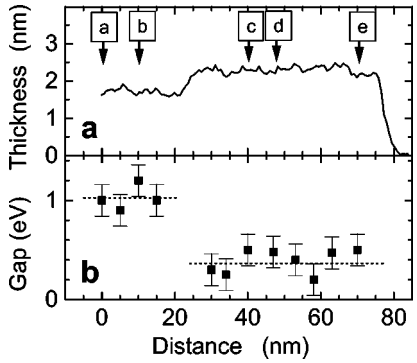


FIG. 2. (a) A cross-sectional profile of the STM image along the *A*-*B* line in Fig. 1(b). (b) Energy gap measured at different points along the *A*-*B* line in Fig. 1(b). The dashed lines indicate the average value of the measured gap.

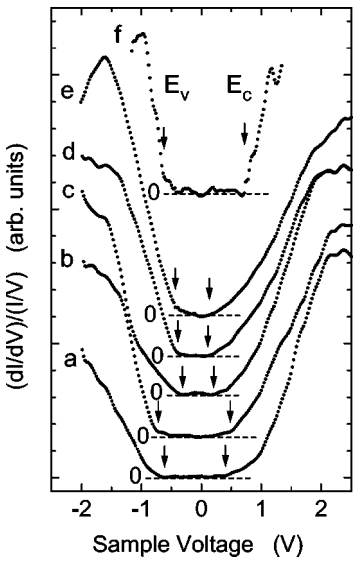


FIG. 3. Normalized differential conductance $(dI/dV)/(I/V)$ spectra of the ErP island (a)–(e) taken at different points on the flat region indicated in Fig. 1(b) and of the InP(001) buffer layer (f). Conduction- and valence-band edges are indicated by arrows.

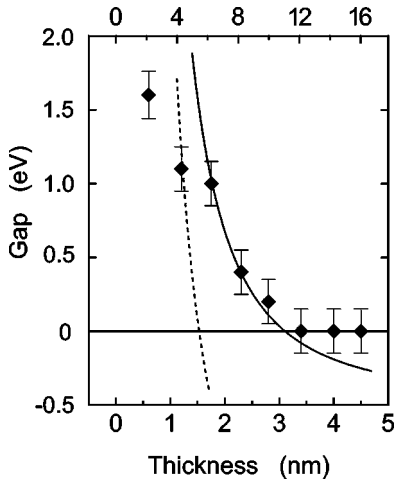


FIG. 4. Energy gap as a function of ErP island thickness. The dashed and solid curves show the calculated dependence assuming a one-dimensional square-well potential with infinite barriers.

intersection of straight lines drawn through the $(dI/dV)/(I/V)$ spectra at the onset energies. In the experiments done by Feenstra, random errors were $\pm 0.03$ eV and systematic errors due to tip-induced band bending were less than 0.1 eV.[22] Figure 3 shows $(dI/dV)/(I/V)$ spectra measured at different points on the two flat regions [Fig. 1(b)] and the InP buffer layer. The spectrum taken at the InP buffer layer yields a gap of $1.4 \pm 0.1$ eV, which agrees with the InP band gap at room temperature (1.35 eV). The slightly large gap obtained here is due to band-bending effects of the buffer layer.

The spectra (a)–(e) taken at the ErP island exhibit a gap, and the magnitude depends on the position. The gap energies measured at the points (a) and (b) are 1.0 and 1.2 eV, respectively, and 0.5 eV for the points (c), (d), and (e). The gap energies measured at different points are summarized in Fig. 2(b). The measured gaps are 0.2-0.5 eV for the flat region with height of 2.30 nm, and 0.9-1.2 eV for the region with height of 1.75 nm. Averaging the measured values over each flat region, the average gaps are $0.4 \pm 0.15$ eV for the thickness of 2.30 nm and $1.0 \pm 0.15$ eV for the thickness of 1.75 nm. Although the accuracy in determination of the gap is $\pm 0.15$ eV, we can obtain an average gap of an island with a certain thickness from the $(dI/dV)/(I/V)$ spectra measured at various points of the island.

To investigate a variation of the average gap with thickness we measured $(dI/dV)/(I/V)$ spectra choosing flat regions with different thicknesses. The thickness dependence of the gap is shown in Fig. 4. For the thickness larger than 3.4 nm no gap is observed in the $(dI/dV)/(I/V)$ spectra. With decreasing thickness the gap increases from 0 eV to $\sim 1.5$ eV. The existence of the energy gap and its thickness dependence suggest opening of a gap depending on the thickness.

We first discuss residual strain effects on the energy gap because there exists a tensile strain due to the lattice mismatch of $+4.67\%$. The misfit strain is partially released by generation of dislocations and voids, and the residual strain is about 2–4 % depending on the growth conditions.[20] The gap change due to the misfit strain can be estimated using a pressure coefficient of the band gap and the elastic moduli. Unfortunately, these parameters of ErP are not known, and thus we use the parameters for GaP, which has a similar band structure except for the semiconducting band gap: the valence-band top at $\Gamma$ point and the conduction-band bottom at $X$ point of the Brillouin zone.[23] The estimated value of the gap increase is 0.06–0.11 eV for the tensile strain of 2–4 %. As the gap change for ErP is expected to be of the same order of magnitude, the strain effect on the observed gap is negligible.

The strong dependence of the gap on the thickness in the range 0.5–3.4 nm suggests QSE on electron and hole states of the semimetal band structure. We calculate confinement sublevel energies of electrons and holes using a square-well potential model taking into account electron and hole Fermi energies.[2] As the lateral size of the flat region is of the order of 50 nm and is much larger than the thickness (1-4 nm), we can use a one-dimensional square-well potential with infinite barriers. The energy gap between the electron sublevel and the hole sublevel $(n=1)$ is given by

$$E_g = \Delta\left(\frac{d_o^2}{d^2} - 1\right),$$

where $\Delta$ is the overlap between conduction and valence bands in the bulk semimetal, and $d_o = \pi\hbar/\sqrt{2\mu\Delta}$ is the critical thickness at which the overlap vanishes. $d$ is the island thickness and $\mu$ is the reduced mass. We use effective masses of the conduction and valence bands along the $\Gamma$-$X$ symmetry line in the Brillouin zone. The momentum distribution of electrons injected from the STM tip is sharply forward peaked; the wave vector parallel to the surface is nearly zero. Considering an epitaxial growth of the rock-salt structure on the InP(001) surface, the {100} surface of the ErP overlayer is grown parallel to the InP(001) surface. Therefore, the properties as measured on the {100} surface by STS are dominated by the energy band along the $\Gamma - X$ line. As the band structure of ErP has the conduction-band minimum

at the $X$ point and the valence-band maximum at the $\Gamma$ point, the size quantization takes place on the dispersion along the $\Gamma - X$ line. The effective masses in this direction obtained by the band calculation are 1.71 $m_o$ and 0.14 $m_o$ for electrons and holes, respectively.[24] The effective masses of ErAs with the similar band structure obtained by the same calculation agree well with the experimental values.[25] Therefore, the calculated masses can be used for the calculation of sublevel energies. The experimental value of the band overlap is not known, but the band calculation provides a band-overlap value of $-1.24$ eV , for ErP. The calculated overlap of ErAs is $-1.41$ eV which is larger than the value (about $-1$ eV) estimated using ultraviolet photoelectron spectroscopic data.[26] As the reliable value of the overlap is not known, we take the band overlap $\Delta$ as an adjustable parameter in the calculation of QSE.

We show in Fig. 4 the calculated gap as a function of thickness taking the values of 1.24 eV and 0.3 eV as $\Delta$. If we use the theoretically calculated overlap (1.24 eV) the critical thickness (1.5 nm) is much smaller than the experiment ($\sim 3$ nm) and the dependence cannot be reproduced as shown by the dashed curve. However, if we take the overlap of 0.3 eV, the theoretical calculation shows an excellent agreement with the observed critical thickness and the dependence in the range 1.7–2.8 nm. The discrepancy seen for $d < 1.2$ nm comes from the finite barrier potential of ErP/InP interface and the change in the effective masses. Although the barrier potential is infinite on the vacuum side, the finite potential at the ErP/InP interface limits the increase in the gap. As the wave vector goes further away from the band extrema, the effective mass becomes large. The strong confinement of electrons and holes in very thin islands cannot be explained by the simple model with assumption of the constant effective mass. There is another possibility that the islands for $d < 1.2$ nm (4 ML) have a different crystal structure and the bands are strongly perturbed by the environment. The misfit dislocations and stacking faults affect electronic states of the ErP layer. As a result, the electronic states of these islands may be strongly modified.

In summary, we have observed the change in the energy gap of the ErP islands (20–50 nm in size) with thickness. The normalized differential conductance spectra indicate a transition from semimetal to semiconductor behavior for the islands with a thickness of $\sim 3$ nm. The observed thickness dependence agrees well with the calculation of QSE using the one-dimensional square-well potential model. These results clearly demonstrate a semimetal to semiconductor transition and a possibility to tailor band gap and carrier concentrations in a semimetal/semiconductor heterostructure by the quantum size effect.

The author (L.B.) would like to acknowledge A. N. Titkov of the A. F. Ioffe Institute, Russia, for continuous encouragement during this study. This paper was supported in part by a Grant-in-Aid for Scientific Research on Priority Areas from the Ministry of Education, Science, Sport and Culture of Japan.

[1] A. Kawabata and R. Kubo, J. Phys. Soc. Jpn. **21**, 1965 (1966).
[2] V. B. Sandomirskii, Zh. Éksp. Teor. Fiz. **52**, 158 (1967) [Sov. Phys. JETP **25**, 101 (1967)].
[3] L. Esaki and L. L. Chang, Phys. Rev. Lett. **33**, 495 (1974).
[4] R. Dingle, W. Wiegmann, and C. H. Henry, Phys. Rev. Lett. **33**, 827 (1974).
[5] See, for example, G. Bastard, Superlattices Microstruct. **1**, 265 (1985).
[6] C. Weisbuch and B. Vinter, *Quantum Semiconductor Structures* (Academic Press, Inc., New York, 1991); M. Reed and W. Kirk, *Nanostructures and Mesoscopic Systems* (Academic Press, Inc., San Diego, 1991).
[7] S. Takatani and Y. W. Chung, Phys. Rev. B **31**, 2290 (1985).
[8] E. Y. Lee, H. Sirringhaus, and H. von Kánel, Phys. Rev. B **50**, 5807 (1994).
[9] G. P. Lopinski, V. I. Merkulov, and J. S. Lannin, Phys. Rev. Lett. **80**, 4241 (1998).
[10] J. W. G. Wildóer, L. C. Venema, A. G. Rinzler, R. E. Smalley, and C. Dekker, Nature (London) **391**, 59 (1998).
[11] B. I. Halperlin and T. M. Rice, Solid State Phys. **21**, 115 (1968).
[12] C. J. Sprindt, R. Cao, K. E. Miyano, I. Lindau, W. E. Spicer, and Y.-C. Pao, J. Vac. Sci. Technol. B **8**, 974 (1990).
[13] A. Guivarćh, J. Caulet, and A. Le Corre, Electron. Lett. **25**, 1050 (1989).
[14] Y. Fujiwara, N. Matsubara, J. Yuhara, M. Tabuchi, K. Fujita, N. Yamada, Y. Nonogaki, Y. Takeda, and K. Morita, in *Compound semiconductors 1995*, edited by Jong-Chun Woo and Yoon Soo Park, IOP Conf. Proc. No. 145 (Institute of Physics, London, 1996), p. 149.
[15] L. Bolotov, J. Tsuchiya, Y. Fujiwara, Y. Takeda, and A. Nakamura, Jpn. J. Appl. Phys., Part 2 **36**, L1534 (1997).
[16] Y. Takeda, K. Fujita, N. Matsubara, N. Yamada, S. Ichiki, M. Tabuchi, and Y. Fujiwara, J. Appl. Phys. **82**, 635 (1997).
[17] M. Tabuchi, K. Fujuta, J. Tsuchiya, Y. Fujiwara, and Y. Takeda, Appl. Surf. Sci. **130-132**, 393 (1998).
[18] R. J. Hamers, R. M. Tromp, and J. E. Demuth, Phys. Rev. Lett. **56**, 1972 (1986).
[19] L. Wang, M.E. Taylor, and M.E. Welland, Surf. Sci. **322**, 325 (1995).
[20] L. Bolotov, J. Tsuchiya, Y. Fujiwara, Y. Takeda, and A. Nakamura, Jpn. J. Appl. Phys., Part 1 **38**, 1060 (1999).
[21] R. J. Hamers, in *Scanning Tunneling Microscopy and Spectroscopy: Theory, Techniques and Applications*, edited by Dawn A. Bonnell (VCH Publishers, New York, 1993), p. 78.
[22] R. M. Feenstra, Phys. Rev. B **50**, 4561 (1994).
[23] J. R. Chelikowsky and M. L. Cohen, Phys. Rev. B **14**, 556 (1976).
[24] A. G. Petukhov, W. R. L. Lambrecht, and B. Segall, Phys. Rev. B **53**, 4324 (1996).
[25] R. Bogaerts, F. Herlach, A. De Keyser, F. M. Peeters, F. DeRosa, C. J. Palmstøm, D. Brehmer, and S. J. Allen, Jr., Phys. Rev. B **53**, 15 951 (1996).
[26] C. Wigren, L. Ilver, J. Kanski, P. O. Nilsson, and U. O. Karlsson, Surf. Rev. Lett. **5**, 299 (1998).